J Mater Sci (2007) 42:2126–2131
DOI 10.1007/s10853-006-1235-9

# Synthesis, phase formation study and magnetic properties of $CoFe_2O_4$ nanopowder prepared by mechanical milling

**R. Sani · A. Beitollahi · Yu. V. Maksimov · I. P. Suzdalev**

Received: 3 September 2005 / Accepted: 8 February 2006 / Published online: 15 December 2006


**Abstract** In this work we report the phase formation and magnetic properties of $CoFe_2O_4$ nanopowder prepared by mechanical alloying technique using metallic cobalt and hematite powder (1:1 molar ratio) as the initial raw material in ambient air atmosphere. The formation of single phase cobalt ferrite of $(Co^{2+}_{0.18}\ Fe^{3+}_{0.82})[Co^{2+}_{0.82}\ Fe^{3+}_{1.18}]O_4$ stoichiometry was confirmed for the samples milled above 15 h without any heat-treatment by XRD and Mössbauer techniques. The average crystallite size of the sample milled for 30 h was ~13 nm. The highest room temperature value of the magnetization measured at 1.5 T was 51 e.m.u/g for the sample milled for 25 h which was much lower than the corresponding value of the bulk cobalt ferrite (80.8 e.m.u/g at 300 K) due to the size effect.

## Introduction

The synthesis of spinel ferrite nanoparticles has been investigated intensively in recent years because of their potential applications in high-density magnetic recording, microwave devices and magnetic fluids [1, 2]. Cobalt ferrite ($CoFe_2O_4$) amongst various spinel type ferrites is an interesting magnetic material because of its very high magneto crystalline anisotropy accompanied by a reasonable saturation magnetization. The bulk material of $CoFe_2O_4$ is known to be a typical oxide compound with a spinel structure having a lattice constant å = 8.395 Å [3]. The saturation magnetization of this compound at 5 K is 93.9 e.m.u/g and 80.8 e.m.u/g at 300 K [4]. Various techniques have been developed to prepare nanosized cobalt ferrite particles such as co-precipitation [5], sol-gel [6], hydrothermal [7] and mechanical alloying [8]. Mechanical alloying/activation techniques lend itself very advantageous for the synthesis of various alloys and oxide compounds including electroceramic materials [9]. Of course, measures should be taken regarding the introduction of impurities during milling process. Successful synthesis of $CoFe_2O_4$ nanoparticles was reported using a combination of chemical precipitation, mechanical alloying and subsequent heat treatment by Y.Shi et al [10]. We, based on our knowledge for the first time, however, report here the phase evolution and magnetic properties of $CoFe_2O_4$ nanoparticles prepared by mechanical alloying technique using metallic cobalt and hematite powder as the initial raw materials in ambient air atmosphere.

R. Sani · A. Beitollahi (✉)
Nanomaterial Research Group,
Department of Metallurgy and Materials Engineering,
Iran University of Science and Technology,
Narmak, FarjamTehran, Iran
e-mail: beitolla@iust.ac.ir

Yu.V. Maksimov · I. P. Suzdalev
Semenov Institute of Chemical Physics RAS,
Moscow, Russia

## Experimentals

The starting raw materials were $\alpha$-$Fe_2O_3$ (> 99% purity, Merck, Germany) and Co (> 99% purity, Merck, Germany) powders. Mixture of Co and $\alpha$-$Fe_2O_3$ powders with a molar ratio of Co to $\alpha$-$Fe_2O_3$ 1:1 were loaded together with 10 mm diameter stainless steel

grinding balls into a cylindrical hardened stainless steel vial 50 mm in diameter and 10 mm in length. The ball to powder weight ratio (BPR) was 10:1. The mechanical alloying was performed in a Spex 8000 high-energy vibratory mill for a maximum of 30 h. The activated powders were collected after 1, 5, 15, 25 and 30 h of milling. Phase development in the samples was monitored using a Philips X-ray diffractometer (XRD) with Cu-$K_{\alpha 1}$ radiation in the $2\theta$ angle range between 20 and 100 degrees. The lattice parameters were calculated using Nelson-Riley (N-R) extrapolation method. In this method the magnitude of the lattice parameter ($a$) was found by plotting ($a$) against N-R function: $\left(\frac{\cos^2\theta}{\sin\theta}\right) + \left(\frac{\cos^2\theta}{\theta}\right)$, which approaches zero as $\theta$ approaches 90 degree. Further, extra pure silicon powder (99.99%) was also used as an internal standard in these experiments. The errors of estimation of the calculated lattice parameters were about ± 0.002 Å. The average crystallite sizes of the milled samples were also determined from the full-width at half maximum (FWMH) of the strongest reflection, the (311) peak using the Williamson-Hall method [11] after applying the standard correction for instrumental broadening. Room temperature Mössbauer spectra were recorded on a conventional gamma-resonance spectrometer operating in constant-acceleration mode with $^{57}$Co(Cr) as source. Isomer shifts (IS) are reported relative to α-Fe at room temperature. The spectra were computer-analyzed using the standard program. Room temperature magnetic measurements were carried out using a vibrating sample magnetometer at a maximum field of 1.5 T.

## Results and discussion

### XRD data

Figure 1 shows XRD multiplot pattern of $Co/Fe_2O_3$ powder blend mechanically activated for 0.0, 1, 5, 15, 25 and 30 h. As expected prior to mechanical activation, the powder mixture exhibited sharp crystalline peaks related to metallic Co and hematite (α-$Fe_2O_3$) phases. For the samples milled above 1 h, almost all of previously observed sharp diffraction peaks vanished. The pronounced broadening observed for various diffraction peaks (Fig. 1) could be related to the significant refinement in crystallite and particle sizes of the constituting powders, increase of defect concentration, as well as the formation of some solid solution compounds. For the sample milled for 1 h, although XRD pattern could not clearly detect the formation of trace amounts of $CoFe_2O_4$ phase formed but the

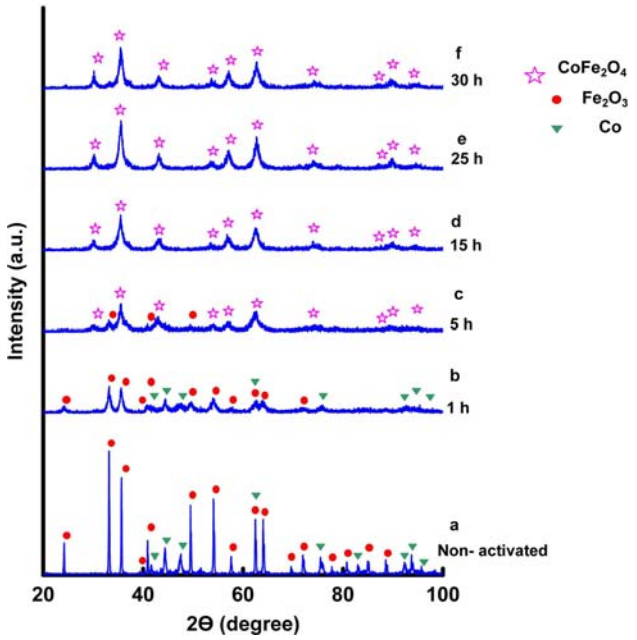


**Fig. 1** XRD multiplot patterns of $Co/Fe_2O_3$ powder blend mechanically activated for 0 h (**a**), 1 h (**b**), 5 h (**c**), 15 h (**d**), 25 h (**e**) and 30 h (**f**)

Mössbauer spectra obtained confirmed the existence of this phase in this sample (Fig. 2 and Table 1). Increasing the milling time to 5 h gave rise to the appreciable increase of the level of formation of cobalt ferrite phase and the disappearance of the main diffraction peak of metallic cobalt powder (Fig. 1c). However, the XRD pattern obtained for this sample confirmed the existence of some non-reacted hematite phase of appreciably smaller average crystallite size (17 nm) compared to that of the initial iron oxide (average particle size 0.5 μm) used as the starting raw material. Furthermore, increasing the milling time to above 5 h, i.e., 15, 25 and 30 h, caused a noticeable increase of the intensities of the diffraction peaks related to cobalt ferrite phase at the expense of the reduction of those of α-$Fe_2O_3$ phase and the only major phase observed was $CoFe_2O_4$ for these samples, within the detection accuracy limit of XRD technique.

Mechanical milling introduces high energy into the material being processed. This energy can be stored in the material as atomic disorder and/or grain boundaries. Additionally, grain refinement increases the grain boundary area and this also raises the free energy of the system. The sum of the energy of these two effects i.e., disordering and creation of grain boundaries will be the total energy introduced into the material during milling. Further, considering the two primary classes of point defects i.e., vacancies and interstitials if there is sufficient activation energy

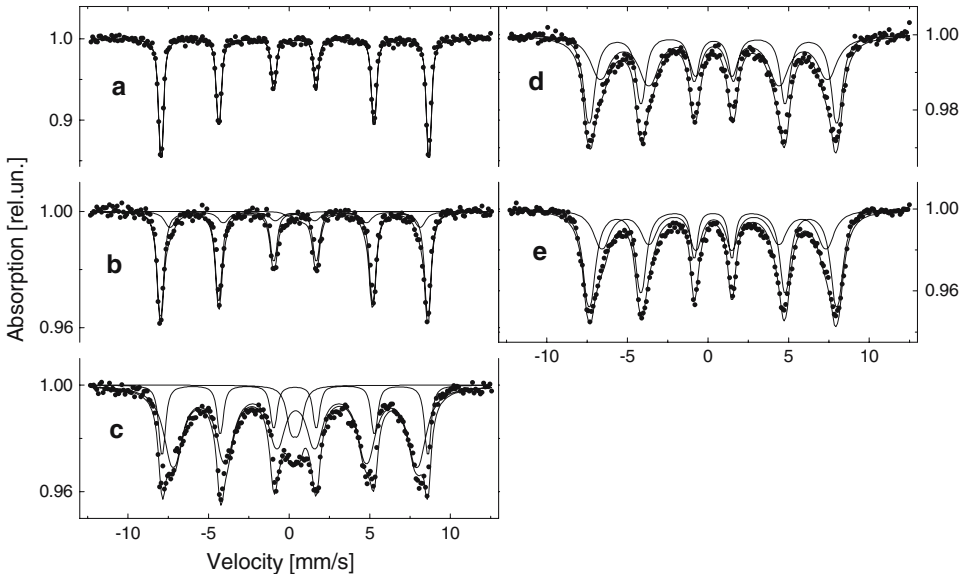


**Fig. 2** Room temperature Mössbauer spectra of various samples milled for 0 h (**a**), 1 h (**b**), 5 h (**c**), 25 h (**d**) and 30 h (**e**) in ambient atmosphere

**Table 1** Mössbauer parameters of the Fe sites for the samples milled for 0, 1, 5, 25 and 30 h (IS–isomer shift, relative to α-Fe; QS-quadruple splitting; $\varepsilon_Q$-quadruple shift; Γ-line width, $H_{in}$–internal magnetic field, $s_A/s_B$ is the area ratio of the tetrahedral and octahedral lines)

| Hours | Fe sites | IS | QS | $\varepsilon_Q$ | Γ | $H_{in}$, ± 0.5T | Rel. cont., ± 0.05 | $s_A/s_B$ |
|---|---|---|---|---|---|---|---|---|
| | | ±0.03 MM/c | | | | | | |
| 0 | α-$Fe_2O_3$ | 0.38 | – | 0.20 | 0.28 | 51.6 | 1.00 | – |
| 1 | α-$Fe_2O_3$ | 0.35 | – | 0.18 | 0.40 | 51.3 | 0.78 | – |
| | $Fe^{3+}$: $CoFe_2O_4$ | 0.36 | – | 0.04 | ~0.70 | 47.8 | 0.20 | – |
| | $Fe^{3+}$ (paramag.)[a] | 0.34 | 0.88 | – | 0.60 | – | 0.02 | – |
| 5 | α-$Fe_2O_3$ | 0.38 | _ | 0.21 | 0.40 | 51.2 | 0.19 | – |
| | $Fe^{3+}$: $CoFe_2O_4$ | 0.39 | – | 0.04 | ~1.20 | 47.0 | 0.74 | – |
| | $Fe^{3+}$ (paramag.)[a] | 0.38 | 0.45 | – | 0.60 | – | 0.07 | – |
| 25 | $Fe^{3+}$ (B): $CoFe_2O_4$ | 0.32 | – | 0.02 | 0.66 | 47.8 | 0.59 | 0.69 |
| | $Fe^{3+}$ (A): $CoFe_2O_4$ | 0.34 | – | 0.02 | 1.20 | 43.5 | 0.41 | |
| 30 | $Fe^{3+}$ (B): $CoFe_2O_4$ | 0.31 | – | 0.01 | 0.65 | 47.8 | 0.59 | 0.69 |
| | $Fe^{3+}$ (A): $CoFe_2O_4$ | 0.34 | – | 0.02 | 1.00 | 43.0 | 0.41 | |

[a] The signal, most probably, arises from superparamagnetic component.

present, atom can move in crystal lattices from one atomic site to another. When dislocations move along a slip plane, the mechanical energy is transformed into kinetic energy of the atoms, which excites the translational mobility of the atoms. All atoms receive additional energy and mobility. As a result of the formation of large amounts of defects due to high-energy collision of the powder particles, the total activation energy required by diffusion is lower because part of the activation energy required to form vacancies may or may not be required completely. Further, during the milling process the rise of defect concentration will give rise to the increase of diffusivity $D$:

$$D = D_o \exp\left(\frac{-\Delta Q}{RT}\right) \quad (1)$$

Where $D_O$ is a material constant, $\Delta Q$ is the activation energy, $R$ is the universal gas constant and $T$ is the temperature.

In addition, or alternatively, the increase in the free energy may promote transition to less thermodynamically stable crystalline phase in compounds that show polymorphism. The energy of any stress field formed can change in to heat which, in turn initiate chemical reaction and lead to the annealing of some defects. For the samples prepared in this work, considering the presence of air atmosphere in the vial and the rise of local temperature of the powder during the balls contact events, one could possibly postulate the in situ oxidation of metallic cobalt to its oxide form and its simultaneous inter-diffusion into the α-$Fe_2O_3$ phase giving rise to the formation of cobalt ferrite phase. The

postulation of simultaneous oxidation of metallic cobalt powder and its instantaneous inter-diffusion in to hematite phase is based on the fact that our XRD results did not revealed any evidences of cobalt oxide formation for the samples subjected to various milling time in this study. This assumption, however, demands further study and justification by using other techniques such as transmission electron microscopy (TEM) for the samples milled for less than 1 h (currently underway).

Figure 3 demonstrates the lattice parameter variations versus milling time for the cobalt ferrite phase formed. As can be realized from this figure, the lattice parameter declined for the samples milled up to 25 h and again increased for the samples milled above this period. The observed trends in this graph could be related to the complex variations of atomic site occupancy, concentration of structural defects, levels of stresses introduced and the degree of crystallinity of the cobalt ferrite formed during the milling process.

Figure 4 displays the variations of the average crystallite sizes of the cobalt ferrite phase formed versus the milling time. As can be realized from this figure, increasing the milling time from 5 h to 30 h gave rise to a rather linear increase of the average crystallite sizes of this compound. A similar crystallite size rise due to the increase of milling time is also previously reported for magnetite samples prepared by mechanical alloying technique [12].

The observed increase of the average crystallite sizes of the formed cobalt ferrite is possibly related to the increased injection of energy and diffusion rate of previously formed nuclei [13]. The formation of structural defects and disorder induced by mechanical activation will favor diffusion and atomic rearrangements at considerably low temperatures. The reaction rates are influenced by the initial contact area and diffusion of the reactant species through the product

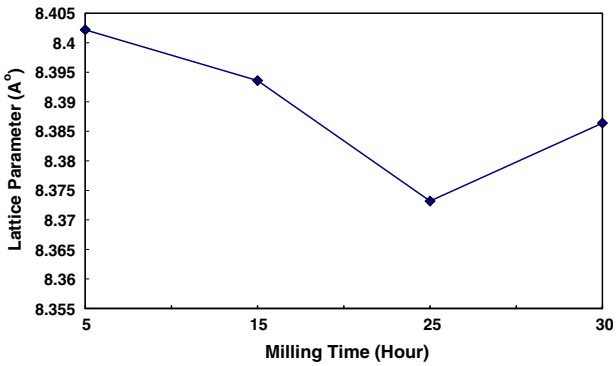


**Fig. 3** Variations of lattice parameter versus milling time for cobalt ferrite phase

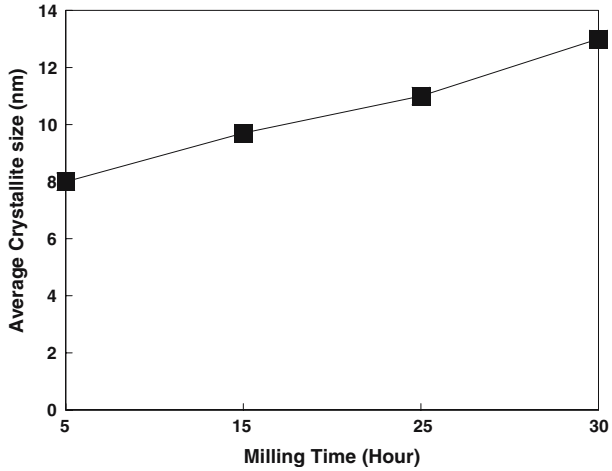


**Fig. 4** Average crystallite size variation of $CoFe_2O_4$ phase versus the milling time

phases [14]. For most solid-state processes, the initial contact area is fixed and diffusion rate is limited. This is not the case for the reactions induced by mechanical activation. Further, a reaction can actually increase with increase in mechanical activation duration and change of phases [15, 16]. Considering that diffusion process during mechanical activation is a dynamic process one can assume that the inter-diffusion layer is broken by the activation process, thus enabling new surfaces with very different compositions to contact each other. Therefore, repeated fracturing and rebinding enlarge the diffusion area, resulting in the enhancement of the diffusion kinetics. Mechanical activation minimizes the effect of product barriers on the reaction kinetics and provides the condition required for the promulgation of solid-state reaction at low temperatures.

## Magnetic data

Figure 5(a) and 5(b) display the room temperature M-H loops as well as the variations of the measured magnetization at 1.5 T and intrinsic coercive field ($_iH_C$) versus the milling time respectively. For the non-activated sample (0 h milled) the magnitudes of the measured magnetization at 1.5 T and $_iH_C$ parameters were 27 e.m.u/g and 100 Oe, which are related to the presence of metallic cobalt powder used. As can be seen in Fig. 5(b) increasing the milling time gave rise to the increase of the measured magnetization at 1.5 T as well as $_iH_C$.

The magnitude of the latter showed a sharp rise for the samples mechanically milled up to 25 h. Further, the observed rising trend for the measured magnetization at 1.5 T with increasing milling time is due to the increased rate of formation of cobalt ferrite as

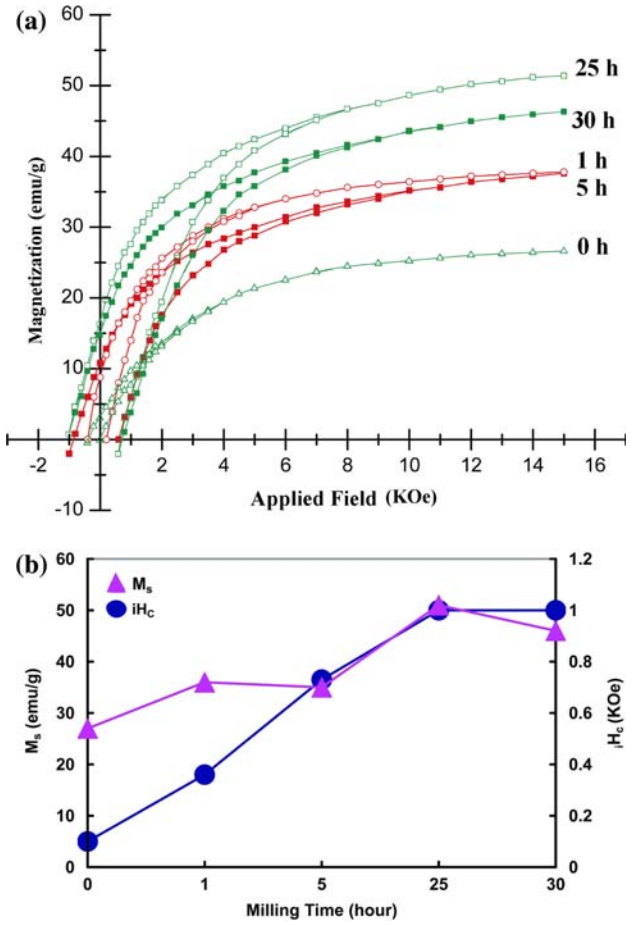


**Fig 5.** Room temperature (M-H) loops (**a**) as well as the variations of the measured magnetization at 1.5 T and intrinsic coercive field ($_iH_C$) of the activated powders at various milling time (**b**)

confirmed with XRD (Fig. 1) and Mössbauer results (Fig. 2 and Table 1). However, it should be mentioned that the rate of increase of magnetization is influenced by the volume fraction of $CoFe_2O_4$ phase formed. The highest value of magnetization measured at 1.5 T (51 e.m.u/g) was obtained for the sample milled for 25 h. This value is much lower than that of the bulk cobalt ferrite (80.8 e.m.u/g at 300 K). The lower values obtained for our nanocrystalline $CoFe_2O_4$ powders could be attributed to the structural distortions in the surface compared to the bulk [17]. The net magnetic moment is reduced in ultra fine particles as the surface has significantly large surface to volume ratio. Thus a large proportion of metal ions are in structurally distorted particle surface, where in, the bond lengths, and bond angles would be different compared to the bulk to give reduced magnetic moment. It is also likely that the cation site occupancy in nanosized $CoFe_2O_4$ could be different from the bulk to give reduced magnetic moment [18].

## Mössbauer data

Figure 2 shows room temperature Mössbauer spectra of the samples obtained at various milling periods. The results of computer fittings of the spectra are summarized in Table 1. The spectrum in Fig. 1a was found to be similar to the typical spectra normally seen for polycrystalline hematite ($\alpha$-$Fe_2O_3$) coarse grain particles. Mössbauer spectra of the sample milled for 1 h revealed the coexistence of hyperfine structure (HFS) lines arising from $\alpha$-$Fe_2O_3$ as well as two new sub spectra; HFS lines with relative content 0.2 that may belong to octahedral B-sites of $CoFe_2O_4$ [19] and weak ''paramagnetic'' doublet. The presence of the latter suggests the presence of superparamagnetic particles in the powder mixture. Increasing the milling time for 5 h (Fig. 2c), led to the progressive diminishing of signals from hematite phase with an accompanied increase of the relative content of nanosized $CoFe_2O_4$ phase in agreement with XRD results.

The presence of a complex hyperfine structure in which a quadrupole doublet is superimposed on a magnetically split sextet suggest that these samples (milled for 1 and 5 h) can be possibly divided in to two components of superparamagnetic and ferrimagnetic due to size distribution. Superparamagnetism is characteristic of small crystallites, where in, the magnetization is not fixed in any of the easy axes. It is a consequence of the magnetic spins fluctuating among the easy axes of magnetization in the absence of an external magnetic field. The average time taken for the change of magnetization from one axis to another is the superparamagnetic relaxation time ($\tau$). Both the crystallite size and temperature determines the relaxation time, $\tau$ which is approximated as $\tau = \tau_0 \exp(KV/k_BT)$ where K is the anisotropy constant of the crystallite, V, the crystallite volume, $k_B$, the Boltzman constant and T is the temperature, $\tau_0$ is a constant ($10^{-10}$ s). When temperature is constant, the relaxation time varies as a function of crystallite volume, V and shows changes in the Mössbauer spectra. Further, the essential broadening of the A-sites in the spectra 1d and 1e (Fig. 2) may be interpreted as being due to a random distribution of hyperfine fields caused by the distribution of Co and Fe nearest B-site neighbors. Another reason for line broadening is the disorder in $CoFe_2O_4$ resulting from the random site occupancy of magnetic $Fe^{3+}$ ions by magnetic $Co^{2+}$ ions during ball milling. For the samples milled above 5 h i.e. 25 and 30 h the contribution of super paramagnetic component were found to be negligible. This was also in agreement with the obtained calculated crystallite sizes for these samples. The average crystallite sizes of the samples milled for 15, 25 and 30 h

were above the critical superparamagnetic size reported earlier for $CoFe_2O_4$ nanopowder [20]. It is also interesting to note that the magnitude of the relative content (Table 1) of the hematite phase for the sample milled for 5 h was about 4 times less than that of the sample milled for 1 h which was also in agreement with XRD results. Similar spectra (Fig. 2d, e) were obtained for the samples milled for 25 and 30 h where only two superimposed six-line hyperfine spectra belonging to tetrahedral (A) and octahedral (B) sites of $CoFe_2O_4$ were seen. It is noteworthy that the values of internal hyperfine fields $H_{in}(A)$ ~43.2 T and $H_{in}(B)$ ~47.8 T (Table 1) are less than the corresponding values reported for quenched bulk $CoFe_2O_4$; $H_{in}(A) = 47.2$ T and $H_{in}(B) = 49.4$ T [19]. The observed differences could be related to the particle size effect. The calculated $s_A/s_B$ ratio, which is the area ratio of the tetrahedral to octahedral lines, was found similar (0.69) for the samples milled for 25 and 30 h. These ratios are proportional to the ratio of the number of A- and B-site iron ions assuming the recoilless fraction *f* is the same for the two sites. It should be noted that the value $s_A/s_B = 0.69$ is close to the previously reported value for the quenched sample of $CoFe_2O_4$ ($s_A/s_B = 0.65$) [19]. The cation distribution in case of the samples milled for 25 and 30 h using the mixture of metallic cobalt and polycrystalline hematite prepared in this work is therefore suggested to be considered as: $(Co^{2+}_{0.18}\,Fe^{3+}_{0.82})[Co^{2+}_{0.82}\,Fe^{3+}_{1.18}]O_4$, where $s_A/s_B = 0.69$.

## Conclusions

The below mentioned conclusions were withdrawn based on the work presented here:

1. Single phase $CoFe_2O_4$ ferrite nanopowder was formed by mechanical milling of a powder blend mixture of metallic cobalt and hematite (Co/$\alpha$-$Fe_2O_3$ molar ratio 1:1) above 15 h using a high energy vibratory mill.
2. Mössbauer spectroscopy analysis confirmed the coexistence of superparamagnetic and ferrimagnetic particles for the samples milled for 1 and 5 h.
3. The highest room temperature value of magnetization measured at 1.5 T was 51 e.m.u/g for the sample milled for 25 h which is much lower than that of the bulk cobalt ferrite (80.8 e.m.u/g at 300 K). This is believed to be related to the structural distortions on the surface of cobalt ferrite nanopowder.
4. The stoichiometry of the cobalt phase formed was estimated to be $(Co^{2+}_{0.18}\,Fe^{3+}_{0.82})[Co^{2+}_{0.82}\,Fe^{3+}_{1.18}]O_4$ , based on our Mössbauer analysis.

**Acknowledgements** We would like to acknowledge the help of Iran University of Science and Technology (IUST) during the PhD program of one of the authors (R. Sani). We also like to acknowledge the help of Semenov Institute of Chemical Physics (SICP) RAS, Moscow, Russia, Prof. I.P. Suzdalev and Dr. Yu.V. Maksimov from SICP for their kind help regarding Mössbauer analysis carried out. Finally, we also thank the kind help of Prof. N. Kudervatykh from Institute of Physics and Applied Mathematics, Ural State University, Russia, Ekaterinburg, for his kind help regarding magnetic measurements.

## References

1. Goldman A (1990) In modern ferrite technology. Van Nostrand Reinhold, New York
2. Berkovsky BM, Medvedev VF, Krakov MS, (1993) In magnetic fluids: engineering applications, Oxford University Press, Oxford
3. Bate G, Wohlfarth EP (ed) (1980) Ferromagnetic materials, vol 2. North-Holland, Amsterdam, p 431
4. Pauthenet R, (1952) Ann Phys 7:710
5. Pillai V, Shah DO, (1996) J Magn Magn Mater 163:243
6. Lee JG, Lee HM, Kim CS, Oh YJ, (1998) J Magn Magn Mater 177:181
7. Dvies KJ, WellsS, Upadhyly RV, Charles SW, Grady KO, El Hilo M, Meaz T, Morup S, (1995) J Magn Magn Mater 149:14
8. Ding J, Mccormik PG, Street R, (1995) Solid State Commun 95:31
9. Junmin X, Wang J, Weiseng T, (2000) J.Alloys Compd 308:139
10. Shi Y, Ding J, Yin H, (2000) J Alloys Compd 308:290
11. Williamson GK, Hall WH, (1953) Acta Metall 1:22
12. Dutta S, Manik SK, Pal M, Pradhen SK, Brahma P, Chakravorty D, (2005) J Magn Magn Mater 288:301
13. Beitollahi A, Moravej M, (2004) J Mat Sci 39:1
14. Schaffer GB, Mccormik PG, (1992) Mechanical Alloying Mater.Forum 16:91
15. Mccormic PG, Wharton VN, Royhail MM, Schaffer GB, (1991) In: Microcomposite And Nanophase Materials Tm Warrendale Pennsylvania p 65
16. Lu L, Lai MO, Zhang S, (1994) Mater Week 94:522
17. Kodama RH, (1999) J Magn Magn Mater 200:359
18. Chinnasamay CN, Narayanasamy A, Ponpandian N, Chattopadhayay K, Guerault H, Greneche JM, (2000) J Phys Condens Matter. 12:7795
19. Sawatzky GA, Van Der Woude F, Morrish AH, (1969) Phys Rev 187:747
20. Kim YIL, Kim D, Lee CS, (2003) Physica B 337:42